

Analysis of the performance characteristics of the five-channel Microtops II Sun photometer for measuring aerosol optical thickness and precipitable water vapor

Charles Ichoku,^{1,2} Robert Levy,^{1,2} Yoram J. Kaufman,² Lorraine A. Remer,² Rong-Rong Li,^{1,2} Vanderlei J. Martins,^{2,3} Brent N. Holben,⁴ Nader Abuhassan,^{1,4} Ilya Slutsker,^{1,4} Thomas F. Eck,^{4,5} and Christophe Pietras⁶

Received 18 September 2001; revised 26 November 2001; accepted 20 December 2001; published 12 July 2002.

[1] Five Microtops II Sun photometers were studied in detail at the NASA Goddard Space Flight Center (GSFC) to determine their performance in measuring aerosol optical thickness (AOT or $\tau_{a\lambda}$) and precipitable column water vapor (W). Each derives $\tau_{a\lambda}$ from measured signals at four wavelengths λ (340, 440, 675, and 870 nm), and W from the 936 nm signal measurements. Accuracy of $\tau_{a\lambda}$ and W determination depends on the reliability of the relevant channel calibration coefficient (V_0). Relative calibration by transfer of parameters from a more accurate Sun photometer (such as the Mauna-Loa-calibrated AERONET master Sun photometer at GSFC) is more reliable than Langley calibration performed at GSFC. It was found that the factory-determined value of the instrument constant for the 936 nm filter ($k = 0.7847$) used in the Microtops' internal algorithm is unrealistic, causing large errors in $V_{0(936)}$, τ_{a936} , and W . Thus, when applied for transfer calibration at GSFC, whereas the random variation of V_0 at 340 to 870 nm is quite small, with coefficients of variation (CV) in the range of 0 to 2.4%, at 936 nm the CV goes up to 19%. Also, the systematic temporal variation of V_0 at 340 to 870 nm is very slow, while at 936 nm it is large and exhibits a very high dependence on W . The algorithm also computes τ_{a936} as $0.91 \tau_{a870}$, which is highly simplistic. Therefore, it is recommended to determine τ_{a936} by logarithmic extrapolation from τ_{a675} and τ_{a870} . From the operational standpoint of the Microtops, apart from errors that may result from unperceived cloud contamination, the main sources of error include inaccurate pointing to the Sun, neglecting to clean the front quartz window, and neglecting to calibrate correctly. If these three issues are adequately taken care of, the Microtops can be quite accurate and stable, with root-mean-square (rms) differences between corresponding retrievals from clean calibrated Microtops and the AERONET Sun photometer being about ± 0.02 at 340 nm, decreasing down to about ± 0.01 at 870 nm. *INDEX TERMS:* 0305 Atmospheric Composition and Structure: Aerosols and particles (0345, 4801); 0394 Atmospheric Composition and Structure: Instruments and techniques; 0634 Electromagnetics: Measurement and standards; 1610 Global Change: Atmosphere (0315, 0325); *KEYWORDS:* atmosphere, aerosol, water vapor, Microtops, Sun photometer, calibration

1. Introduction

[2] Aerosols are an enigmatic yet indispensable component in global climate studies and modeling. The physical

characteristics, composition, abundance, and spatial distribution and dynamics of aerosols are still very poorly known. Aerosol spectral optical thickness (AOT or $\tau_{a\lambda}$) and precipitable water vapor amount (W) are two very important physical parameters for characterizing aerosols. Routine observation of total atmospheric column AOT and W globally is a fundamental way of determining aerosol optical characteristics and its influence in the global radiation budget and climate change. The most practical means of making these observations is by remote sensing, which can be either from the ground (looking in the skyward direction with Sun photometers) or from space (looking toward the ground through the atmosphere with imaging radiometers onboard satellites or high altitude aircraft).

[3] Ground-based and satellite remote sensing of AOT and W have different but complementary characteristics.

¹Science Systems and Applications Inc., Lanham, Maryland, USA.

²Laboratory for Atmospheres, NASA Goddard Space Flight Center, Greenbelt, Maryland, USA.

³Joint Center for Earth Systems Technology (JCET), University of Maryland–Baltimore County, Baltimore, Maryland, USA.

⁴Laboratory for Terrestrial Physics, NASA Goddard Space Flight Center, Greenbelt, Maryland, USA.

⁵Goddard Earth Sciences and Technology (GEST) Center, University of Maryland–Baltimore County, Baltimore, Maryland, USA.

⁶Science Applications International Corporation–General Sciences Corporation, NASA Goddard Space Flight Center, Greenbelt, Maryland, USA.

Ground-based observations enable the acquisition of data as many times as possible in one day, but only for individually discrete locations. On the other hand, satellite observations can cover more extensive areas of the earth (even the whole earth) in one day, though only one or two observations can be made on a given position each day. Ground and satellite observations are vital for different situations as well as for cross-validating each other.

[4] A number of currently available operational satellite sensors (for example, AVHRR, TOMS, and more recently MODIS) provide data for retrieving aerosol optical properties. On the other hand, there are a number of networks of ground-based Sun photometers measuring AOT and W at different locations around the world. One such prominent network is the AEROSOL ROBOTIC NETWORK (AERONET) comprising a series of automatic tracking Sun photometers currently occupying more than 100 locations in different parts of the world [Holben *et al.*, 1998, 2001]. Data acquired by AERONET instruments are very widely used by the aerosol community for different kinds of studies and modeling, as well as for the validation of satellite retrievals [Goloub *et al.*, 1999; Zhao *et al.*, 2002]. Specifically, AERONET data is used intensively for the validation of aerosol parameter retrievals from the Moderate Resolution Imaging Spectroradiometer (MODIS) onboard the Terra Satellite launched on 18 December 1999 [Chu *et al.*, 2002; Ichoku *et al.*, 2002; Remer *et al.*, 2002]. However, AERONET Sun photometers cannot be located everywhere and every time AOT and W data are needed, such as during some field campaigns and other special events, as well as for routine measurements applied to certain specific studies. Therefore, there is great need for alternative (especially portable and low-cost) Sun photometers for such purposes.

[5] One of such Sun photometers, which has been used quite widely in recent times is the MICROTOSPS II Sun photometer manufactured by the Solar Light Company, Philadelphia, USA. It is relatively affordable, portable, and easy to operate, and is convenient for all the purposes mentioned above. In fact, MICROTOSPS II has two versions: (i) the ‘ozone monitor’ or ‘ozonometer’ adapted to column ozone measurement and, (ii) the ‘Sun photometer’ designed for aerosol optical thickness measurements. Either one can be configured by the manufacturer to measure water vapor column thickness W . Morys *et al.* [2001] gave a general description of the MICROTOSPS II instrument design, calibration and performance, but focused the discussion on the ozonometer type. Although, they discussed the water vapor retrieval aspects, they admitted that ‘the column water vapor measurements by MICROTOSPS II have yet to be fully analyzed’ [Morys *et al.*, 2001, p. 14,581]. Porter *et al.* [2001] examined the use of the Sun photometer version of the MICROTOSPS II onboard ship platforms, and possible effects of instability caused by ship motion on the measurement accuracy. However, their instruments do not include the 936 nm (water vapor absorption) channel, and does not measure W . Therefore, it has become imperative to fully characterize the Microtops II Sun photometer in order to determine its reliability in acquiring $\tau_{a\lambda}$ and W data, especially for use in satellite data validation. This is the objective of this study.

2. Instrument Description and Operation

[6] The Microtops II Sun photometer is a portable instrument, measuring 10 cm by 20 cm by 4.3 cm, and weighing only 600 grams [Morys *et al.*, 2001]. It is designed for use as a hand-held manually operated instrument. The physical and operational characteristics of the instrument are detailed in the ‘‘User’s Guide,’’ which is publicly accessible on the Internet (<http://www.solar.com/manuals.htm>). The Sun photometer measures solar radiance in five spectral wave bands from which it automatically derives AOT. The five wavelengths may be specified while ordering the instrument, such that appropriate filters are custom designed and installed by the manufacturer.

[7] In this study, five Microtops II Sun photometers (serial numbers: 3761, 3762, 3763, 3760, and 3657) of exactly the same type have been used. Each has five channels with peak wavelengths, λ , of 340, 440, 675, 870, and 936 nm. The filters used in all channels have a peak wavelength precision of ± 1.5 nm, and a full width at half maximum (FWHM) band pass of 10 nm (<http://www.solar.com/sunphoto.htm>). It is pertinent to mention that the 936 nm wavelength is greatly affected by water vapor absorption. As such, the most significant parameter used to derive W in the instruments is the 936 nm signal data.

[8] At 340, 440, 675 and 870 nm wavelengths, AOT is derived based on the Beer-Lambert-Bouguer law as follows:

$$V_{\lambda} = V_{0\lambda} D^{-2} \exp(-\tau_{\lambda} M) \quad (1)$$

where, for each channel (wavelength),

- V_{λ} = the signal measured by the instrument at wavelength λ ,
- $V_{0\lambda}$ = the extraterrestrial signal at wavelength λ ,
- D = Earth-Sun Distance in Astronomical units at time of observation,
- τ_{λ} = total optical thickness ($\tau_{\lambda} = \tau_{a\lambda} + \tau_{R\lambda} + \tau_{O3\lambda}$) at wavelength λ ,
- $\tau_{a\lambda}$ = aerosol optical thickness (AOT) at wavelength λ ,
- $\tau_{R\lambda}$ = Rayleigh (air) optical thickness at wavelength λ ,
- $\tau_{O3\lambda}$ = Ozone optical thickness at wavelength λ ,
- M = the optical air mass

Because of the nonlinear contribution from water vapor in the 936 nm channel, the equivalent equation for this channel is given by [e.g., Reagan *et al.*, 1995]:

$$V_w = V_{0w} D^{-2} \exp[-\tau_w M - k(WM)^b] \quad (2)$$

where,

- V_w , V_{0w} , D , τ_w , and M remain as defined in equation (1), except that subscript w is used to designate the 936 nm water vapor absorption channel.

W = vertical water vapor column thickness

k and b are instrument constants numerically derived for the 936 nm filter.

The Rayleigh and Ozone optical thicknesses, τ_R and τ_{O3} , are obtained from atmospheric models:

$$\tau_{R\lambda} = R_4 \exp(-h/29.3/273) \quad (3)$$

$$\tau_{O3\lambda} = Ozabs * DOBS/1000 \quad (4)$$

Table 1. Values of Rayleigh Optical Thickness ($\tau_{R\lambda}$) and Ozone Absorption Cross Section ($Ozabs$) Computed for the Site of the Experiment: Latitude Equal to 39.033°, Longitude Equal to -76.883°, and Elevation Equal to 50 m

	Wavelength, nm				
	340	440	675	870	936
$\tau_{R\lambda}$	0.705	0.241	0.042	0.015	0.011
$Ozabs$	0.039	0.0034	0.0414	0.0036	0

where,

h = altitude of the place of observation in meters

$$R_4 = 28773.6 * (R_2 * (2 + R_2) * \lambda^{-2})^2$$

$$R_2 = 10^{-8} * \{8342.13 + 2406030 / (130 - \lambda^{-2}) + 15997 / (38.9 - \lambda^{-2})\}$$

λ = wavelength in microns

(For further information on $\tau_{R\lambda}$ computation, see, e.g., Edlén [1966], Teillet [1990], and Bodhaine et al. [1999].)

$Ozabs$ = Ozone absorption cross section, extracted from a lookup table based on wavelength [e.g., Molina and Molina, 1986; Vigroux, 1953],

$DOBS$ = Ozone amount in Dobson units, extracted from a lookup table based on latitude and date of observation [e.g., London et al., 1976].

[9] The precipitable water vapor column thickness W is evaluated by combining equations (1) and (2), and making W the subject of the resulting equation [e.g., Morys et al., 2001]. As described in the MICROTOS II User’s Guide [Solar Light Company, Inc., 2000], the derivation of AOT in the Microtops instruments does not take into account the Ozone component of the optical thickness. It assumes that this effect is negligible. Table 1 shows a listing of $\tau_{R\lambda}$ and $Ozabs$ computed for our place of observation, which has an elevation of about 50 m above sea level. It is obvious that $\tau_{R\lambda}$ is quite substantial, especially in the lower wavelengths. Also, given that the values of $DOBS$ range between 240 and 440, substituting it in equation (4) would yield $\tau_{O3\lambda}$ values of the order of 30% of the $Ozabs$ values in Table 1. Although the $\tau_{O3\lambda}$ values are small, they are certainly not negligible, especially at 340 and 675 nm wavelengths.

[10] The omission of Ozone corrections in the Microtops computation of AOT is one reason to study the instrument measurement characteristics and calibration requirements. Another reason is that, in the Microtops, τ_w (i.e. τ_{a936}) is computed as $0.91 \tau_{a870}$ even though it is acknowledged in the user’s guide that equation (2) is the appropriate relationship. Furthermore, any errors that may be incurred from these two inadequate computations would likely propagate into the evaluation of W . All these provide solid justifications for a detailed study of the instrument.

3. Methodology

3.1. Experimental Design

[11] Several Microtops II Sun photometers are currently used in the various aerosol-related projects at the National Aeronautics and Space Administration (NASA), Goddard Space Flight Center (GSFC), Greenbelt, Maryland. The instruments are from time to time deployed in the field for data acquisition when necessary in different parts of the world. Most of the data is intended for use in validating

aerosol retrievals from MODIS and other satellite sensors. To achieve reliable validation, it is imperative to know the performance characteristics of each instrument. As such, a series of measurements have been conducted occasionally at GSFC with these instruments since 1997 alongside a reference instrument, which is the master automatic tracking Sun photometer/sky radiometer (CIMEL Electronique 318A) belonging to AERONET [Holben et al., 1998]. In its regular operational mode, approximately every 15 minutes during the daytime, the AERONET master Sun photometer in GSFC takes direct Sun measurements from which it derives $\tau_{a\lambda}$ (at 340, 380, 440, 500, 670, 870, and 1020 nm wavelengths) and W . It also takes sky radiance measurements hourly for computing certain other aerosol parameters such as size distribution. For Sun measurements, the AERONET master instrument at GSFC is regularly calibrated by Langley plots at the pristine mountaintop of the National Oceanic and Atmospheric Administration (NOAA) Observatory at Mauna Loa (MLO), Hawaii, and for sky measurements it is calibrated in the laboratory (with a standard integrating sphere). The MLO-calibrated GSFC AERONET master Sun photometer is adopted as a standard to calibrate many other Sun photometers, including identical types deployed at other locations around the world [Holben et al., 1998, 2001]. It is therefore used for calibrating most Microtops Sun photometers used by GSFC scientists, and is hereafter referred to as the “reference Sun photometer”, “AERONET master Sun photometer,” or simply as “AERONET”.

3.2. Microtops II Sun Photometer Measurements

[12] For this study Microtops II Sun photometer measurements were conducted alongside and concurrently with the reference Sun photometer. During the measurement sessions, each Microtops was used to take a sequence of measurements in quick succession each time the AERONET Sun photometer rises to take its measurements. This is to evaluate the consistency of the Microtops’ measurements, as well as to ensure that one or more of the sequence of measurements is as close in time as possible to the actual moment of the AERONET Sun photometer measurement.

[13] Microtops’ measurements are always taken with great care at GSFC to meet high standards for use in calibration against the AERONET master Sun photometer. First of all, to avoid cloud contamination, Microtops measurements are conducted on days that are as cloud-free as possible, and in any case, when there is no cloud patch covering or even close to the line of sight to the Sun. In fact, all effort is made to maintain at least an angular distance of 30° between the Sun and the closest cloud patch. When possible, measurements are conducted around the local solar transit time (local solar noon) in order to limit the effect of optical distortions due to large solar zenith angles, except when intended for use in obtaining Langley plots as described below. The instruments are operated by persons that have undergone proper orientation beforehand in order to minimize human errors from inaccurate pointing to the Sun. Tests conducted with some of the Microtops revealed that bad pointing to the Sun can erroneously increase the AOT values considerably. The Microtops Sun-centering view window has cross hairs and two concentric circles, all having a common center. Appropriately, if the optics of

Table 2. Original V_0 Values Set by the Manufacturer in Each of the Five Microtops II Sun Photometers Used in This Work

Serial No.	Instrument ID	$V_{0,340}$	$V_{0,440}$	$V_{0,675}$	$V_{0,870}$	$V_{0,936}$
1	3761	3108.825	1246.382	1155.167	788.396	1824.388
2	3762	3074.815	1283.056	1163.281	795.523	1828.041
3	3763	3435.783	1204.717	1174.972	814.032	1483.263
4	3760	3155.808	1199.908	1160.957	832.139	1802.626
5	3657	1848.260	995.256	974.574	729.967	1694.258

the Microtops is completely without fault, when centered, the Sun's center should coincide with the center of the cross hairs and should lie completely inside the inner circle. To test the sensitivity of the instrument to Sun-pointing, the Sun was centered on the circumference of each of the two circles, at the four points where each circle is intersected by a cross hair. Two Microtops Sun photometers (serial numbers 3761 and 3762) were used in this test. At the time of the test, with correct Sun centering the average value of τ_{a870} was 0.06, but when the Sun was deliberately centered at the intersections of the cross-hair and the inner circle the average τ_{a870} was 0.9, while for the outer circle it was 3.0. This shows that centering the Sun's image away from the optical axis of the instrument increases AOT error in an exponential fashion. However, it could be possible that when the instrument optics is faulty, the center indicated by the cross hairs and circles may be shifted slightly with respect to the true center. Also, being a hand-held instrument, constancy in centering cannot always be achieved, especially when in a moving platform such as a ship [Porter et al., 2001]. For this reason, it is always advisable to take many measurements in quick succession so as to retain only those corresponding to the smallest AOT values, as these would represent measurements from the most accurate Sun pointing.

3.3. Microtops II Sun Photometer Calibration

[14] Table 2 shows the original calibration coefficients set by the manufacturer in each of the 5 Microtops Sun photometers studied in this work. Over time, the calibration coefficients in each instrument may change due to the aging of its optical filters and other influences. The calibration of a Microtops II Sun photometer involves the determination of fresh up-to-date $V_{0\lambda}$ and V_{0w} values, which may then be substituted into equations (1) and (2) to recompute calibrated values of $\tau_{a\lambda}$, τ_{aw} and W . There are two main ways of determining the $V_{0\lambda}$ and V_{0w} values: (i) by independent calibration using the Langley plots technique [e.g., Schmid et al., 1998]; and (ii) by relative or transfer calibration against a more accurate instrument, in this case the MLO-calibrated AERONET Sun photometer.

3.3.1. Langley calibration method

[15] In the Langley method a sequence of measurements is taken with the Microtops during several hours while the solar zenith angle (SZA) or the optical air mass (M) is either decreasing (morning) or increasing (afternoon) continuously. Ideally $\tau_{a\lambda}$ (and indeed τ_{λ}) as well as W should remain constant, or approximately so, throughout each measurement session (morning or afternoon). This is why Langley calibration measurements are often conducted on high altitude locations such as the high mountain top of Mauna Loa, Hawaii [e.g., Dutton et al., 1994; Schmid and Wehrli, 1995; Holben et al., 1998]. The Langley method of calibration is based on the principle of linear relationships

produced from logarithmic transformations of equations (1) and (2). Taking the natural logarithms of both sides of equation (1), one obtains

$$\ln(V_{\lambda}) = \ln(V_{0\lambda}D^{-2}) - \tau_{\lambda}M \quad (5)$$

Equation (5) is a linear equation with slope $-\tau_{\lambda}$ and intercept $\ln(V_{0\lambda}D^{-2})$. To generate Langley plots for each wavelength λ , using the data acquired during each measurement session, $\ln(V_{\lambda})$ is plotted against M . Based on equation (5), a linear least squares fit to the straight part of the Langley plot for each wavelength λ produces the ordinate intercept $\ln(V_{0\lambda}D^{-2})$ from whose exponential the calibration coefficient $V_{0\lambda}$ is evaluated. Similarly, for the 936-nm water vapor absorption band, taking the natural logarithm of both sides of equation (2), one gets

$$\ln(V_w) = \ln(V_{0w}D^{-2}) - \tau_w M - k(WM)^b \quad (6)$$

which, when rearranged, becomes

$$\ln(V_w) + \tau_w M = \ln(V_{0w}D^{-2}) - kW^b M^b \quad (7)$$

where all the variables are as already defined in equation (2). Plotting the left hand side of equation (7) against M^b produces what is known as the modified Langley plot, with slope kW^b and intercept $\ln(V_{0w}D^{-2})$ from whose exponential V_{0w} is evaluated [e.g., Halthore et al., 1997; Schmid et al., 1998]. It is obvious, from equation (7), that τ_{aw} ($\tau_w = \tau_{aw} + \tau_{Rw} + \tau_{O3w}$) is needed to realize the modified Langley plot. Since τ_{aw} is assumed unknown a priori, it is estimated from other parameters. Generally, after determining the $V_{0\lambda}$ values for other wavelengths λ , the calibrated $\tau_{a\lambda}$ values are computed at these wavelengths for all measurement times, and τ_{aw} values are obtained by interpolation from corresponding $\tau_{a\lambda}$ values at neighboring wavelengths [Halthore et al., 1997]. The interpolation is based on the logarithmic relationship of $\tau_{a\lambda}$ to wavelength λ [e.g., Eck et al., 1999], and could be performed using values at two or more channels. However, for the Microtops used, the water vapor absorption band (936 nm) happens to be the highest wavelength, and τ_{aw} could only be obtained by extrapolation (rather than interpolation). This was done using τ_{a870} and τ_{a675} as follows:

$$\tau_{aw} = \tau_{a870} \exp\{\alpha_{870/675} \ln(936/870)\} \quad (8)$$

where,

$$\alpha_{870/675} = \ln(\tau_{a870}/\tau_{a675})/\ln(870/675)$$

Here, $\alpha_{870/675}$ is the Ångström exponent derived using only the 870 and 675 nm channels. Although the Ångström

exponent derivation and the τ_{a^w} extrapolation could have been performed based on all four aerosol channels (340, 440, 675, and 870 nm), using a linear or second order polynomial fit [Eck *et al.*, 1999], it was estimated that the logarithmic relationship between τ_{a^λ} at 675, 870, and 936 nm was sufficiently linear to yield accurate τ_{a^w} values.

3.3.2. Transfer calibration method

[16] This involves the use of data measured concurrently with the Microtops and the reference Sun photometer to generate V_{0^λ} and V_{0^w} calibration coefficients, which may be used to transfer the measurement accuracy of the reference Sun photometer (whose accuracy has been well established) to the Microtops Sun photometer measurements through data adjustment. In this work, for use in calibration, corresponding measurements from the Microtops and the reference instrument are required to be within 30 seconds (in rare cases, up to 60 seconds may be allowed). Several of such data point pairs are acquired in a given calibration measurement session.

[17] If the calibration coefficients V'_{0^λ} and the raw voltage measurements V'_λ of the reference Sun photometer are available, it is possible to substitute these in equation (1), then do similarly with the corresponding V_{0^λ} and V_λ from the Microtops. A ratio of the two resulting equations will eliminate the common parameters leaving only these 4 variables, as follows [e.g., Porter *et al.*, 2001]:

$$V_\lambda/V'_\lambda = V_{0^\lambda}/V'_{0^\lambda} \quad (9)$$

Note that, for this relationship to hold accurately, the central wavelengths of the corresponding channels for the Microtops and the reference Sun photometer must match very closely. The only unknown in equation (9) is V_{0^λ} , which can then be very simply evaluated. However, this simple ratioing procedure cannot be used to derive V_{0^w} with equation (2) because of the parameters, k and b , which are not common to Microtops and AERONET instruments. Therefore, we have resorted to calculating V_{0^λ} and V_{0^w} directly from equations (1) and (2), respectively, using all known parameter values. For each data point pair, the τ_{a^λ} , τ_{a^w} and W values obtained from the reference Sun photometer are substituted together with the Microtops V_λ and V_w measurements into equations (1) and (2) to derive calibrated V_{0^λ} and V_{0^w} values for the Microtops.

[18] Both the ratioing and the direct calculation methods were used to derive V_{0^λ} and the values were compared. The results of the two methods were in close agreement at all four wavelengths (340, 440, 675, and 870 nm). For each wavelength, the agreement followed the same pattern in all five Microtops. The root-mean-square (rms) differences of corresponding V_{0^λ} values between the two methods (computed from all data for the entire experiment) when expressed as percentages of the average original V_{0^λ} values in Table 2 are: 1.12% at 340 nm, 0.27% at 440 nm, 0.43% at 675 nm, and 0.17% at 870 nm, which are almost insignificant.

[19] Calibrated (or adjusted) values of τ_{a^λ} , τ_{a^w} and W for the Microtops Sun photometer can be calculated from equations (1) and (2) using the calibrated V_{0^λ} and V_{0^w} , as well as the Microtops-measured V_λ and V_w values and the instrument constants. Thus, data acquired with Microtops

Sun photometers anywhere may be adjusted to AERONET accuracy based on this principle of calibration transfer.

3.4. Microtops II Sun Photometer Data Adjustment

[20] Microtops AOT and W retrievals are adjusted (or corrected) by using the measured signals V_λ and V_w and the calibrated coefficients V_{0^λ} and V_{0^w} to recompute the parameters τ_{a^λ} , τ_{a^w} and W through the inversion of equations (1) and (2). The process of adjusting data measured with the Microtops Sun photometer at a field location based on transfer-calibration from the AERONET Sun photometer at GSFC has been illustrated in Sabbah *et al.* [2001]. However, regardless of the source of the calibration coefficients, the adjustment procedure is the same and is once again described here for completeness. The calibration coefficients, V_{0^λ} and V_{0^w} , obtained from each calibration season (a period of 30 days or less during which some calibration measurement sessions are conducted) are averaged. The average coefficients for two consecutive calibration seasons are used to adjust all data measured in the intervening period. To achieve this, first, sets of V_{0^λ} and V_{0^w} from consecutive calibration seasons are linearly interpolated with time to compute calibrated sets of V_{0^λ} and V_{0^w} for all the intervening dates and times of regular observations. Then, the interpolated set of V_{0^λ} and V_{0^w} for each time of observation is substituted in equation (1) or (2), to compute the adjusted τ_λ from which the adjusted τ_{a^λ} (or τ_{a^w}) is derived ($\tau_{a^\lambda} = \tau_\lambda - \tau_{R\lambda} - \tau_{O3\lambda}$).

[21] Adjustment for τ_{a^λ} at 340, 440, 675, and 870 nm wavelengths is straightforward using equation (1). For τ_{a^w} (i.e. τ_{a^λ} at 936 nm) and W , the adjustment cannot be done directly with equation (2) because each of them is needed to compute the other. Therefore, a different procedure is used to adjust them. First, the adjusted τ_{a^w} is determined by extrapolation from $\tau_{a^{675}}$ and $\tau_{a^{870}}$ based on equation (8). It should be mentioned that the extrapolation method used here is an improvement over the internal determination of τ_{a^w} in the Microtops II Sun photometer (which is done simply by multiplying $\tau_{a^{870}}$ by the constant 0.91, based on the presumption that $\tau_{a^{936}}$ and $\tau_{a^{870}}$ are always related by this constant [Morys *et al.*, 2001]). Once τ_{a^w} is extrapolated, the adjusted value of W is derived by combining equations (1) and equation (2) and substituting the adjusted $\tau_{a^{870}}$ and τ_{a^w} as well as the other required parameters.

4. Analysis of Results

[22] In this analysis, the MLO-calibrated AERONET master Sun photometer at GSFC is considered as the reference standard. The five Microtops Sun photometers used will be identified by their manufacturer-assigned serial numbers, namely 3761, 3762, 3763, 3760, and 3657. The focus of this discussion will be on the characteristics of the three sets of parameters determined in this work: the retrieved aerosol optical thickness (τ_{a^λ} and τ_{a^w}), the retrieved column precipitable water vapor (W), and the computed calibration coefficients (V_{0^λ} and V_{0^w}).

4.1. Aerosol Optical Thickness (τ_{a^λ} and τ_{a^w})

[23] Figures 1a to 1e show scatterplots of the AOTs measured directly with each of the five Microtops in the

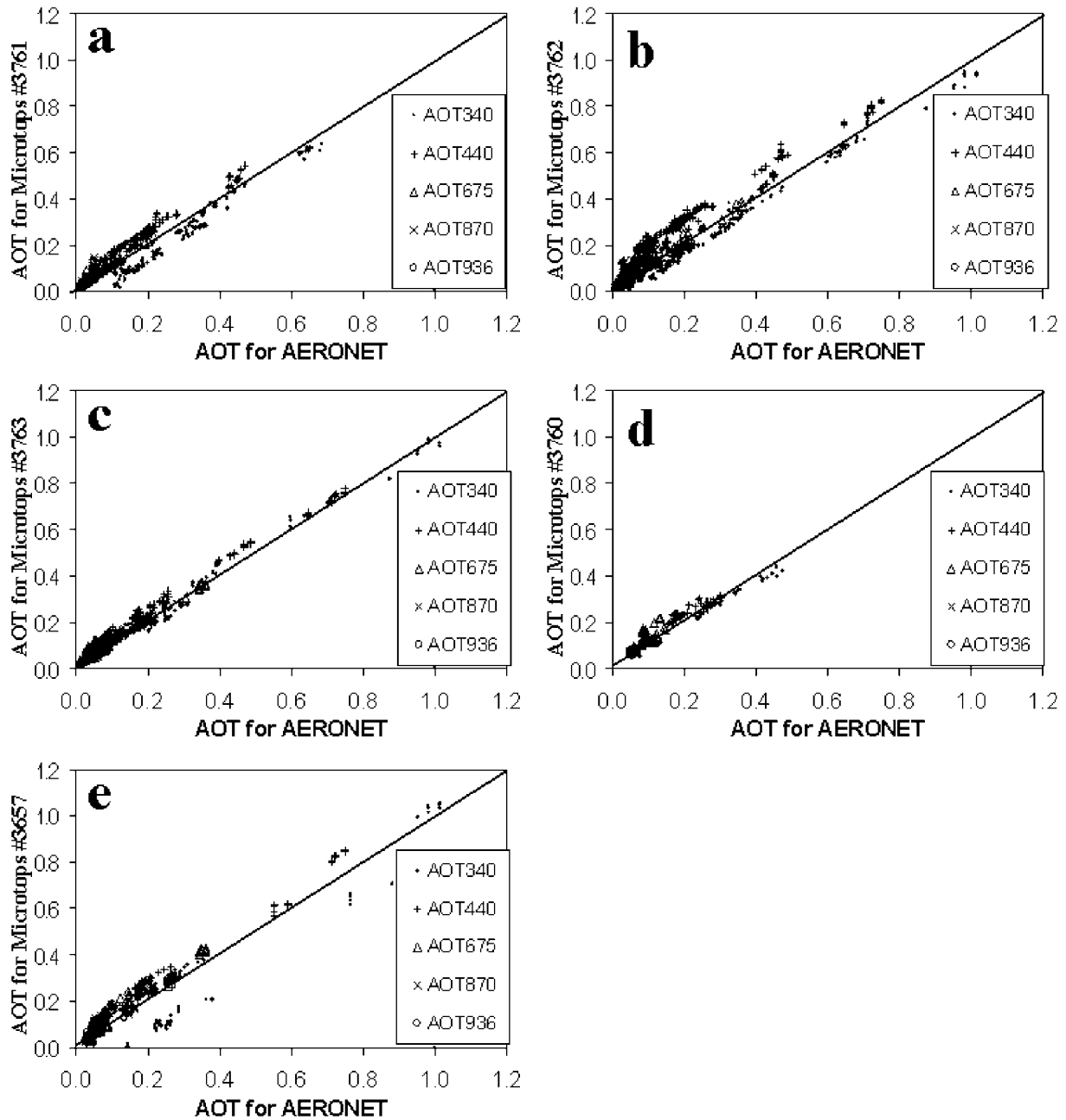


Figure 1. Scatterplots of AOT ($\tau_{a\lambda}$) measured with each of the five Microtops Sun photometers against those of the AERONET (CIMEL) master Sun photometer at NASA-Goddard Space Flight Center (GSFC). The Microtops' measurements are based entirely on their original calibration coefficients as determined by the manufacturer.

five spectral channels (340, 440, 675, 870, and 936 nm) against those of the AERONET Sun photometer. The Microtops data are the raw unadjusted data based on the original calibration coefficients. Note that AERONET does not retrieve AOT at 936 nm (τ_{a936}), but this was interpolated from τ_{a870} and τ_{a1020} using equation (8), with 870 and 1020 substituted for 675 and 870, respectively. The plots include all the Microtops data acquired at GSFC during the entire period of the experiment, regardless of time of day or aerosol concentration. The relationship between the AOTs

from Microtops and AERONET appears to be significantly good for Microtops numbers 3763 and 3760, but not so good for the other three, although overall they are not so bad, given that they are all raw Microtops data based on the original calibration coefficients. Table 3 shows the number of days of observation covered and the total number of observations plotted for each instrument, the slope, intercept, and coefficient of correlation R for the linear regression fits, as well as the root-mean-square (rms) differences between the Microtops and AERONET values. The

Table 3. Linear Regression Variables From Scatterplots of $\tau_{a\lambda}$ and W Between Data Retrieved Over GSFC From Five Microtops II Sun Photometers (y Axis) Against Corresponding AERONET Data (x Axis) Used for Calibration During a Greater Part of the Period From 1997 to 2000

Serial No.	Instrument ID	Data Days	Observations	Variables	$V_{0.340}$	$V_{0.440}$	$V_{0.675}$	$V_{0.870}$	$V_{0.936}$	Water
1	3761	11	222	slope	1.062	0.966	0.985	0.994	1.003	0.601
				intercept	-0.071	0.063	0.026	0.016	0.011	0.310
				R	0.992	0.989	0.982	0.949	0.942	0.982
				rms	0.058	0.059	0.027	0.019	0.015	0.511
2	3762	18	334	slope	0.972	0.951	0.968	0.930	0.970	0.648
				intercept	-0.019	0.110	0.029	0.022	0.016	0.219
				R	0.993	0.986	0.979	0.920	0.916	0.993
				rms	0.038	0.102	0.030	0.025	0.021	0.549
3	3763	13	137	slope	0.978	0.988	0.963	0.917	0.970	0.693
				intercept	0.013	0.048	0.028	0.029	0.022	0.083
				R	0.993	0.993	0.986	0.914	0.918	0.998
				rms	0.030	0.050	0.028	0.030	0.027	0.580
4	3760	5	50	slope	0.890	0.706	0.570	1.208	1.245	0.588
				intercept	0.015	0.101	0.084	0.001	0.000	0.274
				R	0.989	0.920	0.327	0.856	0.914	0.995
				rms	0.025	0.042	0.051	0.020	0.018	0.422
5	3657	9	112	slope	1.051	1.046	1.067	1.141	1.197	0.668
				intercept	-0.071	0.052	0.037	0.017	0.012	0.223
				R	0.946	0.989	0.964	0.912	0.904	0.994
				rms	0.104	0.070	0.052	0.039	0.036	0.616

slopes are close to 1, the offsets close to zero, and the R's close to 1; although this is a little less so for instrument number 3760. This is probably because the data from this instrument is statistically a small sample, having the smallest range of values and covering the fewest number of days. It is obvious from Figure 1 that Microtops #3760 shows a much better agreement with AERONET than Microtops #3657 does, as portrayed by the values of the mean absolute differences.

[24] For all five cases, at most of the wavelengths, the Microtops seem to overestimate AOT slightly with respect to AERONET, except at 340 nm where they seem to underestimate, mostly for smaller AOT values (lower aerosol concentration). One remarkable thing is that for each of the Microtops, the average deviation of points from the line of equality does not increase with the magnitude of AOT (Figures 1a–1e). As such, it can be inferred that, since the average deviation is ‘constant,’ the larger the AOT, the more comparable the values from AERONET and Microtops.

4.2. Water Vapor Column Thickness, W

[25] Figures 2a to 2e show scatterplots for W from the five Microtops against those of the AERONET Sun photometer. Like for AOTs the linear correlation is appreciably good for each instrument. However, the slopes show that the Microtops consistently underestimate W with respect to AERONET (except for a small offset in #3761), with the deviation increasing as the value of W increases. The consistently positive and non-negligible offset shows a type of “dark current” effect for the Microtops, whereby it hypothetically would measure a residual water vapor even if there is none. The interesting feature of the scatterplots in Figures 2a to 2e is that they all seem to be appreciably linear. Apparently, a linear regression fit to each one should provide the linear equation parameters for computing AERONET water vapor, given Microtops water vapor measurements, and

vice versa. The linear equation for such a computation could be of the form

$$W_m = \alpha W_a + \varepsilon \quad (10)$$

where W_m is the (Microtops) measured water vapor, W_a is the adjusted (AERONET standard) water vapor, α and ε are the slope and intercept, respectively (both given in the WATER column of Table 3 for each Microtops Sun photometer studied). Thus, when any of the Microtops measures W_m , the adjusted equivalent W_a can be quite easily computed. Nevertheless, this method of adjustment is artificial and may not address the source of the measurement discrepancy between the AERONET and Microtops Sun photometers. As will be shown in section 4.3, the problem is being traced to probable inaccuracies in the values of, not only V_{0w} , but also the k and possibly b constants as used in equation (2).

4.3. Calibration Coefficients ($V_{0\lambda}$ and V_{0w})

[26] The calibration coefficients $V_{0\lambda}$ (and V_{0w}) play a vital role in determining the accuracy of the parameters ($\tau_{a\lambda}$, τ_{a^w} and W) retrieved from the instrument voltage measurements V_λ and V_w . Therefore, it requires very careful consideration. The evolution of the calibration values in the life of the Microtops can be assessed by analyzing the results of the two (Langley and transfer) calibration methods performed in this work.

4.3.1. Langley calibration

[27] This type of calibration was performed in GSFC during the fall season of the year 2000 using only the three Microtops Sun photometers (numbers 3761, 3762, and 3763), which were available at the time. Table 4 shows the details of the observations and computed parameters. They include instrument numbers, dates, times (UT) at which observations started and ended including corresponding beginning and ending optical air masses (AM), number of observations (No. Obs.), mean AOT at

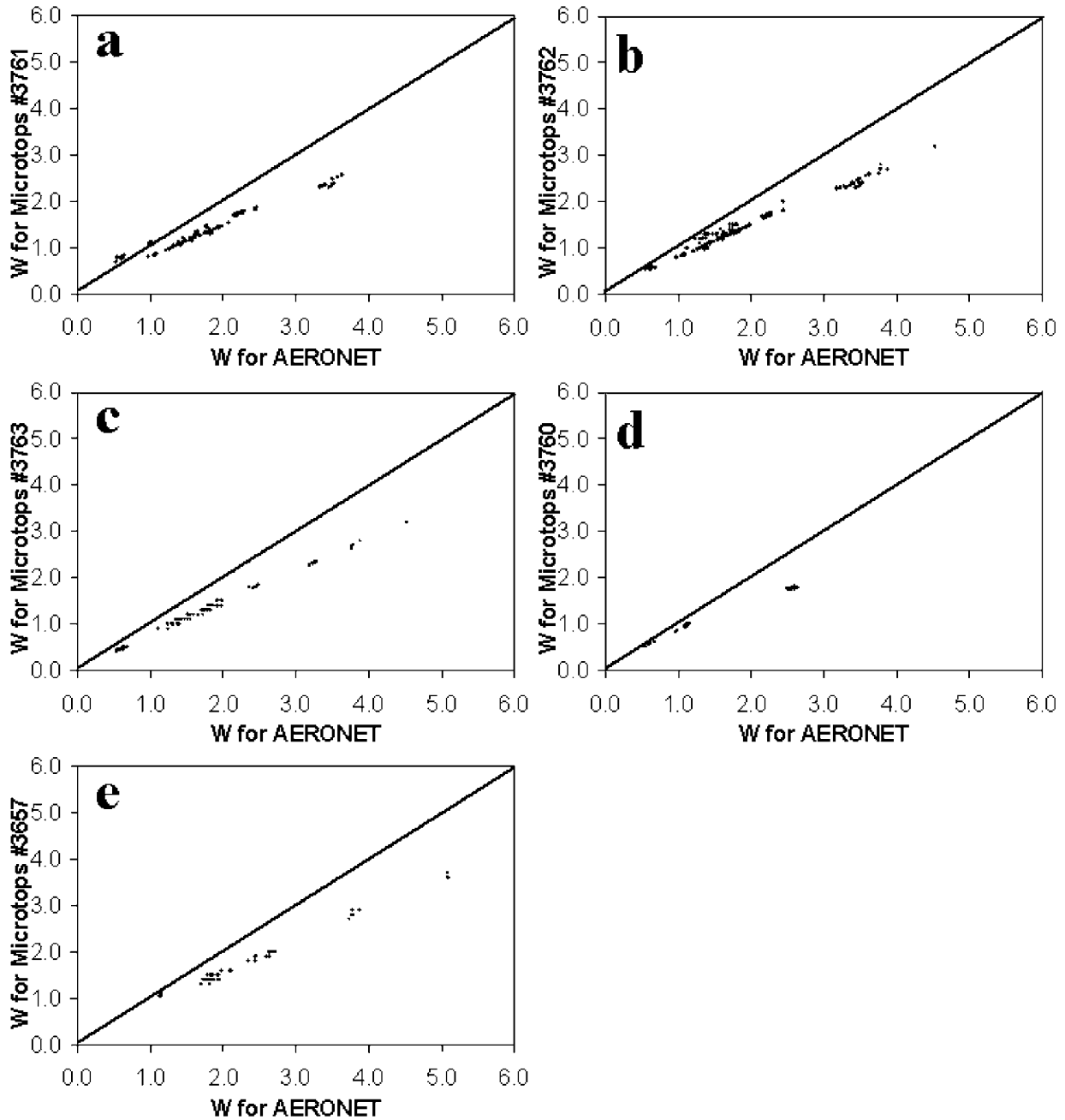


Figure 2. Scatterplots of precipitable water vapor (W) measured with each of the five Microtops Sun photometers against those of the AERONET (CIMEL) master Sun photometer at NASA-Goddard Space Flight Center (GSFC). The Microtops’ measurements are based entirely on their original calibration coefficients as determined by the manufacturer.

675 nm (Mean τ_{a675}), and the derived $V_{0\lambda}$ values for the three Microtops. Only data sets obtained under stable atmospheric conditions (in terms of the apparent aerosol loading and water vapor situations) with air mass range greater than 2 are considered. There are seven of these, numbered serially from 1 to 7 in Table 4 just for ease of identification. Each data point represents a morning or afternoon measurement session for a Microtops instrument. There is only a morning (#2) and an afternoon (#1) data sets for instrument 3761, a morning (#4) and three afternoon

(#3, #5, and #6) data sets for instrument 3762, and only one afternoon (#7) data set for instrument 3763. It is pertinent to mention that most of the data sets for the Langley plots irrespective of wavelength gave a linear regression coefficient R equal to or very close to unity. Out of the 35 determinations (7 sessions of 5 wavelengths) the lowest two R -values were 0.986 and 0.990 while the others range from 0.994 to 1. For each of the two instruments with morning observations, these tend to produce smaller $V_{0\lambda}$ values than their afternoon counterparts, especially at the 340 and

Table 4. Details of Langley Calibration of Three Microtops II Sun Photometers in GSFC^a

Serial No.	Instrument ID	Date	Start Time	Stop Time	Start AM	Stop AM	Observations	Mean $T_{a,675}$	$V_{0,340}$	$V_{0,440}$	$V_{0,675}$	$V_{0,870}$	$V_{0,936}$
1	3761	29-Sep-00	16:59:10	21:40:32	1:340	4:366	80	0.058	3296.958	1130.238	1130.681	781.386	1820.728
2	3761	03-Oct-00	12:39:27	17:13:10	3:410	1:373	36	0.216	3210.493	1096.540	1118.216	766.617	1434.055
3	3762	29-Sep-00	17:13:56	21:41:56	1:343	4:449	73	0.057	3102.066	1095.498	1135.126	791.107	1832.324
4	3762	03-Oct-00	12:33:21	16:57:46	3:638	1:373	37	0.211	2929.813	1023.593	1123.065	768.909	1416.748
5	3762	31-Oct-00	16:53:08	21:30:53	1:674	9:074	253	0.032	3223.264	1095.206	1153.737	792.765	1676.703
6	3762	01-Nov-00	19:45:28	21:08:14	2:589	5:849	132	0.034	3106.406	1058.543	1149.178	785.975	1640.905
7	3763	29-Sep-00	17:44:42	21:40:54	1:370	4:395	75	0.055	3280.995	1127.844	1155.641	803.718	1507.750

^aNote: All times are in Universal Time.

936 nm channels. One probable reason is because incidentally the morning observations generally were conducted over a relatively shorter period of time than those of the afternoon, have fewer samples and smaller air mass ranges, and therefore are probably inadequate for the purpose of deriving $V_{0\lambda}$. If only the afternoon results are used to compare the corresponding original $V_{0\lambda}$ values (Table 2) at 440, 675, and 870 nm wavelengths for the 3 instruments concerned, the calibrated values are generally lower at all three wavelengths, perhaps indicating filter degradation. However, among the three instruments, the marginal difference is largest at 440 nm wavelength. This could indicate that the optical filters at 440 nm undergo degradation faster than those used at other wavelengths. This apparent rapid degradation of the Microtops 440 nm filter was also observed by Porter *et al.* [2001].

4.3.2. Transfer calibration with the AERONET sun photometer at GSFC

[28] During the 3-year period of the experiment, periodically each Microtops Sun photometer was calibrated against the GSFC AERONET Sun photometer based on the transfer method described above. Figures 3a–3e show time series of the percent deviations of the mean calibrated $V_{0\lambda}$ values for each day ($V_{0\lambda}^c$) from the original manufacturer set values ($V_{0\lambda}^o$) shown in Table 2 for each of the five Microtops. The percent deviations were computed as $100 * [(V_{0\lambda}^c - V_{0\lambda}^o) / V_{0\lambda}^o]$. The plots show that calibrated $V_{0\lambda}$ values are appreciably stable at 440, 675, and 870 nm, a little less stable at 340 nm, but quite noticeably unstable at 936 nm. The variability of the 340 nm channel may have been due to a combination of the effects of Rayleigh and ozone absorption as well as the deposit of aerosol on the front quartz window (through which the solar flux enters the Microtops), all of which influence this channel much more than they do others. As regards the 936 nm channel, the superimposed time series of the column water vapor (W) values from AERONET shows that in all cases W has influenced V_{0w} (Vo(936)) very heavily.

[29] With reference to equation (2), although V_w depends on V_{0w} and W , there is no basis for V_{0w} to depend on W . Surprisingly, all the Microtops used here exhibited the dependence of V_{0w} on W . This is an indication that the k and/or b constants (see equation (2)) in these instruments may not be sufficiently accurate. The manufacturer-introduced instrument-constant settings in each of the Microtops used in this study are: $k = 0.7847$ and $b = 0.5945$. Generally, these constants are determined from model calculations using radiative transfer codes such as LOWTRAN or MODTRAN [e.g., Schmid *et al.*, 1996; Halthore *et al.*, 1997]. The k and b constants depend on the geographical latitude and season of the place of interest, but mostly on the wavelength and bandwidth represented by the optical filter in the instrument of interest. As indicated earlier, the filters in the 936 nm channel (as well as the other channels) of the Microtops studied, have a bandwidth of 10 nm FWHM. For a Sun photometer with similar characteristics (946 nm wavelength and 5 nm bandwidth), Schmid *et al.* [1996] used several codes (LOWTRAN7, MODTRAN3, FAS-COD3P, as well as other experimental methods) over different atmospheric categories (midlatitude summer and winter and subarctic winter) and found the overall average values of $k = 0.621 \pm 0.022$ and $b = 0.591 \pm 0.017$. Also Halthore

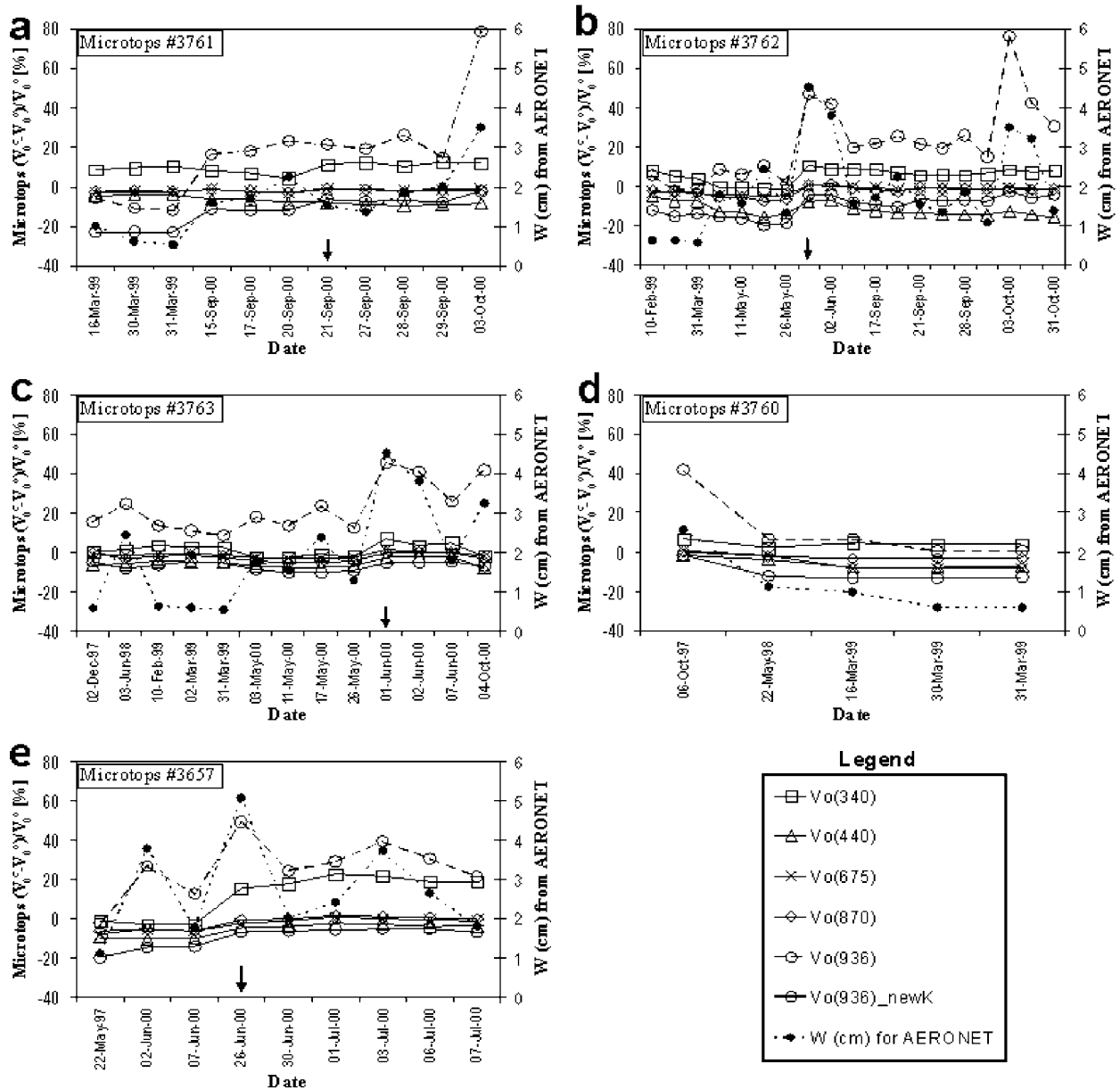


Figure 3. Time series of changes in Microtops calibration coefficients determined by transfer calibration with the AERONET master Sun photometer at GSFC (V_0^c) with respect to the original factory preset values (V_0^o) for the five Microtops. The percent deviations, computed as $[100 * (V_0^c - V_0^o) / V_0^o]$, are based on average V_0^o values for each calibration day. AERONET W data corresponding to the different calibration days are superimposed, to demonstrate the dependence of the 936 nm channel V_0 (i.e. $Vo(936)$) on water vapor. Arrows pointing to the date axes show the date that the first careful cleaning of each instrument was recorded (following a long period of time during which the instrument was either not cleaned or cleaning was not properly done or documented). Note the sudden increase of V_0 values at the time of cleaning. Following a re-evaluation of the instrument constant k , a new set of V_0 values at 936 nm were calculated (with the newly determined value of $k = 0.615$ instead of the original value of 0.7487) and plotted as “ $Vo(936)$ _newK,” which show almost no dependence on water vapor W .

et al. [1997] performed similar calculations for filters with similar characteristics (940 nm wavelength and 10 nm FWHM) using MODTRAN3, for midlatitude winter and summer and tropical atmospheres, and found the overall average values of $k = 0.616$ and $b = 0.594$. It is obvious that the k -values determined from these previous studies are very

close to each other but very different from that used in our Microtops, whereas the b -values are almost equal. Therefore, the k -value used in the Microtops is more likely to be inaccurate. To rectify this situation, a value of k was empirically derived from the Microtops’ calibration data. During transfer calibration, while computing V_{0w} for a

Microtops, the correlation coefficient (R) between the computed V_{0w} and the AERONET W was calculated from the data set representing each calibration season. The k -value was iteratively decremented or incremented until the smallest possible value of R in magnitude (usually $|R| < 0.001$) was obtained, in which case the correlation between V_{0w} and W was virtually eliminated. A weighted mean of all the k -values determined in this way was computed as a more appropriate value for our Microtops. The weight (Ω) for a k -value was determined as follows:

$$\Omega = (W_{\max} - W_{\min}) * (N_{\text{data}} / N_{\text{days}}) \quad (11)$$

where,

Ω is the weight for a k -value,

W_{\max} is the maximum value of W (in cm) from AERONET data,

W_{\min} is the minimum value of W (in cm) from AERONET data,

N_{data} is the number of measured data points used to compute the k -value,

N_{days} is the number of days of measurement for the season. Weights have been computed as shown in equation (11) because the k -values were determined here on the basis of minimum correlation coefficient R between V_{0w} and W . Statistically, the reliability of R is related to the data set range of values (here, $W_{\max} - W_{\min}$) and the number of values (N_{data}). However, to avoid undue influence by the number of data points (N_{data}), these have been normalized by the number of days (N_{days}), resulting in number of data points per day. The final weighted mean k -value determined for our Microtops was $k = 0.615$, which incidentally is very close to those determined for filters of similar characteristics by others [e.g., Schmid *et al.*, 1996; Halthore *et al.*, 1997] as stated above.

[30] The new value of $k = 0.615$ was used to re-compute V_{0w} for all the transfer calibration data. The time series of the V_{0w} based on the new k -value are also shown in Figures 3a–3e (labeled “Vo(936)_newK”). It is obvious that, with the new k -value, V_{0w} (“Vo(936)_newK”) does not follow the trend of W any more but rather conforms to the more natural trends of the $V_{0\lambda}$ curves for the other wavelengths. Even the large error bars located at some points along the old “Vo(936)” curves have practically shrunk away in the corresponding “Vo(936)_newK” curves. To further verify the validity of the new k -value, it was used to re-compute W from measured data, exactly the same way the computation is done in the Microtops, the only difference being just replacing the old k -value with the new one (but retaining everything else, including the original V_{0w}). Scatterplots of both the new and old W against their AERONET equivalent are shown in Figures 4a–4e. Apparently, the correlation has remained unchanged, but the inclination of the data trend against the line of equality has been rectified in each of the plots. Now with the new k -value, in all cases, just like the AOT data in Figures 1a–1e, the average deviation between Microtops and AERONET W data does not change with magnitude.

[31] During a calibration season, at least three suitable data days are required for the calibration to be considered acceptable. The calibration coefficients $V_{0\lambda}$ derived in one season are averaged for use in data adjustment. Table 5

shows the statistics (mean μ , standard deviation σ , mean absolute deviation α , and coefficient of variation $CV = \sigma/\mu$) for all the $V_{0\lambda}$ values determined during each instrument’s last calibration season for this experiment. Also shown are the beginning and ending dates as well as the number of data days and the total number of individual measurements used for calibration during the season. The mean $V_{0\lambda}$ values differ significantly from the corresponding original $V_{0\lambda}$ values (Table 2). Incidentally, at 340 and 936 nm, the mean values are larger than the corresponding original values, while the opposite is the case at the other three wavelengths (440, 675, and 870 nm), which is the expected situation due to instrument filter degradation. The CV values show that the largest instability occurs at the 936 nm channel for all five Microtops, due probably to the tremendous water vapor influence at this wavelength. Thus, whereas the CV values for the other channels fall in the range of 0 to 2.4%, those of the 936 nm channel range from 3.1% to 18.8%.

4.3.3. Behavior of $V_{0\lambda}$

[32] For a given Microtops, two determinations of $V_{0\lambda}$ at a given wavelength (separated even by a very short time) are seldom exactly equal. There is a variation of $V_{0\lambda}$, which has both a random and a systematic component. The random part could be attributed to a variety of common sources, while the systematic change is time dependent and has two aspects. In the first case, if an instrument’s front quartz window is not cleaned over a long period of time, some aerosol would settle on it. Because of this aerosol build-up on the window, which is falsely measured as part of the aerosol in the atmosphere, the $V_{0\lambda}$ values tend to slowly decrease with time. This was the case for all the instruments at the initial stages of the experiment, when their front quartz windows were either not adequately cleaned or not cleaned at all. The systematic decrease of the $V_{0\lambda}$ values was slowly taking place in all the instruments. At some stage, each of the Microtops windows was cleaned thoroughly and the $V_{0\lambda}$ values jumped back up. In Figures 3a–3e, the date on which each instrument was given the first major cleaning is indicated by an arrow. The exception is instrument #3760 (Figure 3d), which was unavailable for cleaning because it had been deployed in the field far away from the site of this experiment. For the other case of time-dependent degradation, even if the quartz window is cleaned regularly, the filters may still undergo degradation, which may be slower but irrecoverable. This natural filter degradation is typical of optical filter-based instruments [e.g., Holben *et al.*, 1998].

[33] One other issue to look into is the differences between the results of the two calibration methods (‘Langley’ and ‘transfer’). Table 6 shows the results of the Langley calibration (already shown in Table 4) together with the mean of the transfer calibration performed with the same data sets. Note that the number of observations used for transfer calibration is always fewer than those used for the Langley plots. This is because, during measurement, readings were taken very frequently with the Microtops and were all used for Langley, but since the reference (AERONET) Sun photometer made observations less frequently, only the Microtops measurements within 30 seconds of the AERONET were used for the transfer calibration. The sessions at which there were no corresponding observations from AERONET have no transfer calibration, and are

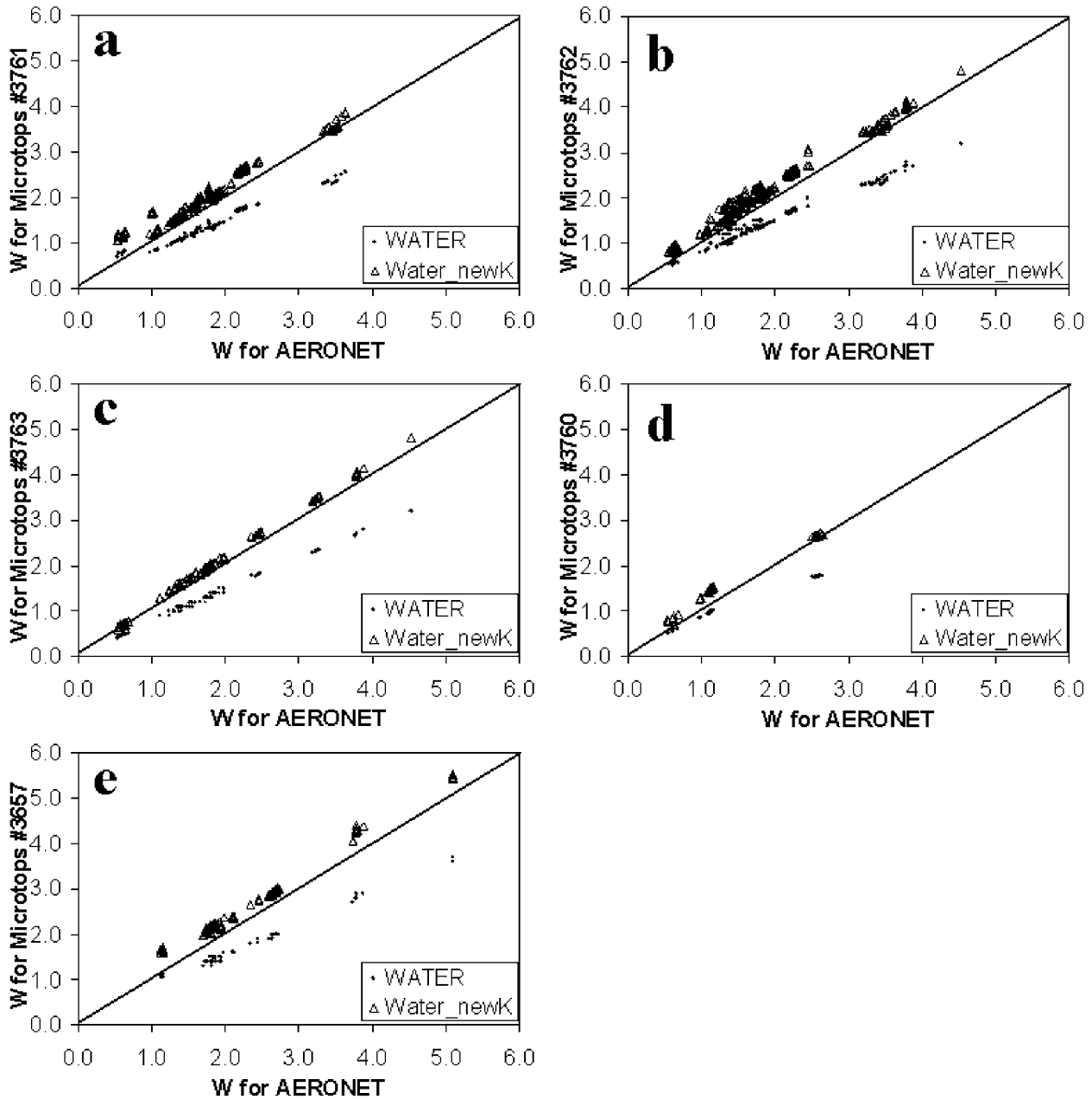


Figure 4. Scatterplots of the Microtops' W databased on the original ($k = 0.7847$) and re-evaluated ($k = 0.615$) values of the instrument constant k against AERONET W data. The same manufacturer-determined V_0 values shown in Table 2 were used in both cases. The new databased on $k = 0.615$ (Water_newK) show no inclination with respect to the 1-to-1 line. Rather, they are only offset to it just like the AOT plots in Figure 1. Like for the AOT plots, the remaining 1-to-1 line offset can now be corrected if calibrated values of V_0 are applied.

designated with N/A (not available) in Table 6. It is obvious from Table 6 that the two calibration methods produced quite considerable differences in $V_{0\lambda}$. However, considering the results of instrument #3762 which has the most data sets, the various transfer calibration values are much closer to one another and, therefore, more consistent than those of the Langley calibration. This could be attributed to the fact that the conditions under which the observations were made are not quite suitable for Langley calibration, which is best under aerosol-free or low and constant aerosol loading

conditions. Furthermore, for transfer calibration the parameter being measured (AOT) is known a priori (from the reference instrument, assuming it meets the required accuracy standard) and the determination expresses the accuracy of the reference Sun photometer. In the case of the Langley method, the AOT is not known and the determined coefficients only express the intrinsic measurement accuracy of the Microtops under the prevailing atmospheric conditions at the time of measurement. Besides, as indicated above, Langley assumes constant AOT for each measurement

Table 5. Statistics (μ is mean, σ is standard deviation, α is mean absolute deviation, CV is coefficient of variation σ/μ) of V_0 Determined During the Last Acceptable Season of Microtops Transfer Calibration Against the AERONET Master Sun Photometer at GSFC^a

Serial No.	Instrument ID	Start Date	Stop Date	Data Days	Observations	Variables	$V_{0,340}$	$V_{0,440}$	$V_{0,675}$	$V_{0,870}$	$V_{0,936}$	$V_{0,936}$
1	3761	21-Sep-00	03-Oct-00	5	129	μ	3471.719	1136.480	1139.163	774.561	2403.790	1711.341
						σ	76.116	12.826	10.015	12.516	452.301	46.421
						α	50.553	7.040	5.339	5.375	317.861	31.081
						CV(%)	2.192	1.129	0.879	1.616	18.816	2.713
2	3762	03-Oct-00	31-Oct-00	3	76	μ	3322.899	1097.907	1146.933	785.211	2788.511	1761.055
						σ	53.001	24.072	8.790	3.766	517.786	41.636
						α	38.519	20.076	6.602	2.932	437.896	29.973
						CV(%)	1.595	2.193	0.766	0.480	18.569	2.364
3	3763	01-Jun-00	07-Jun-00	3	42	μ	3603.866	1180.662	1180.465	814.979	1937.602	1413.016
						σ	87.168	10.962	14.696	7.499	118.729	19.018
						α	72.027	8.857	12.401	6.078	99.547	15.735
						CV(%)	2.419	0.928	1.245	0.920	6.128	1.346
4	3760	16-Mar-99	31-Mar-99	3	17	μ	3293.810	1109.142	1064.501	805.383	1857.055	1568.806
						σ	21.650	4.221	2.703	2.261	57.840	11.458
						α	18.024	3.482	2.487	1.727	53.273	8.811
						CV(%)	0.657	0.381	0.254	0.281	3.115	0.730
5	3657	26-Jun-00	07-Jul-00	6	53	μ	2196.825	960.424	968.985	731.853	2194.516	1600.387
						σ	41.807	9.800	12.120	8.765	124.493	19.740
						α	30.241	7.274	8.681	6.492	86.228	15.765
						CV(%)	1.903	1.020	1.251	1.198	5.673	1.233

^aNotice the difference between the values at the 936 nm channel determined with the manufacturer-specified k value of 0.7847 ($V'_{0,936}$) and those determined with the freshly evaluated k value of 0.615 ($V_{0,936}$). The mean V_0 values, as well as $k = 0.615$, could have been set in the respective instruments, if desired, with effect from the dates shown under the column "Start Date" until the next calibration season.

Table 6. Comparison of Calibration Coefficients V_0 From the Transfer and Langley Methods of Calibration for the Same Time Periods at GSFC^a

Serial No.	Instrument ID	Date	Start Time	Stop Time	Observations	Variables	$V_{0,340}$	$V_{0,440}$	$V_{0,675}$	$V_{0,870}$	$V_{0,936}$
1	3761	29-Sep-00	16:59:10	21:40:32	80	LANGLEY	3296.958	1130.238	1130.681	781.386	1820.728
						TRANSFER	N/A	N/A	N/A	N/A	N/A
2	3761	03-Oct-00	12:39:27	17:13:10	36	LANGLEY	3210.493	1096.540	1118.216	766.617	1434.055
						TRANSFER	3477.908	1141.761	1138.980	774.143	1785.722
3	3762	29-Sep-00	17:13:56	21:41:56	73	LANGLEY	3102.066	1095.498	1135.126	791.107	1832.324
						TRANSFER	3276.234	1095.462	1147.565	785.055	1689.545
4	3762	03-Oct-00	12:33:21	16:57:46	37	LANGLEY	2929.813	1023.593	1123.065	768.909	1416.748
						TRANSFER	3344.289	1120.077	1150.784	787.524	1782.032
5	3762	31-Oct-00	16:53:08	21:30:53	253	LANGLEY	3223.264	1095.206	1153.737	792.765	1676.703
						TRANSFER	3318.489	1076.999	1142.188	783.472	1752.881
6	3762	01-Nov-00	19:45:28	21:08:14	132	LANGLEY	3106.406	1058.543	1149.178	785.975	1640.905
						TRANSFER	N/A	N/A	N/A	N/A	N/A
7	3763	29-Sep-00	17:44:42	21:40:54	75	LANGLEY	3280.995	1127.844	1155.641	803.718	1507.750
						TRANSFER	N/A	N/A	N/A	N/A	N/A

^aNote that for the transfer calibration the values shown are the means of V_0 values computed from individual measurements for the period of the corresponding Langley determinations. N/A designates when data are not available.

session, but this is hardly ever the case. In fact, depending on place of observation, it might be difficult if not impossible to find sufficient number of observation sessions meeting the constant AOT criterion. Thus to calibrate in a location with variable AOT, if a very accurate reference Sun photometer is available, as in our case, it should be preferable to perform transfer calibration rather than Langley calibration. *Weihs et al.* [1995] conducted comparisons between the two calibration methods and obtained similar findings, although their investigation covered only three wave bands, namely 368, 500, and 675 nm.

[34] Based on the trend of the calibration coefficients from the transfer calibrations (Figure 3) it can be inferred that, with the exception of the 936 nm channel, the calibration coefficients of the Microtops at other wavelengths are appreciably stable. However, if the front quartz window is left uncleaned, the coefficients at these other channels undergo degradation, which is a little more pronounced in the 340 nm channel. If a Microtops instrument is cleaned regularly and calibration performed under favorable conditions, average values of coefficients determined during a calibration season can be set in the instrument and should yield regular measurements of acceptable quality until the next calibration season. However, it is recommended that the interval between calibration seasons be of the order of one year or less, depending on instrument usage.

4.4. Sensitivity Analysis of $V_{0\lambda}$ (the Effect of $V_{0\lambda}$ Error on Computed AOT)

[35] It is appropriate to consider quantitatively the effect of error in $V_{0\lambda}$ on computed AOT. Figure 5 shows spectral plots of average AOT values derived with the original Microtops $V_{0\lambda}$ values and those computed from the Langley and transfer calibrations. They are averages of AOT values computed from the data sets corresponding to the various sessions of the Langley calibration as depicted in Table 6. As such, there are no curves for transfer calibration for cases without $V_{0\lambda}$ values in Table 6. The standard deviations of the averaged AOTs are plotted as error bars for each of the sessions, although most of them are very small, and fall inside the point markers. The differences between the various curves in each panel illustrate the effect of using the various $V_{0\lambda}$ values to compute AOT. Note that the curves labeled "Transfer_V0" represent exactly the AOTs measured by the AERONET Sun photometer. If this AERONET curve is assumed accurate, then it is obvious that, in most of the cases, the Microtops measurements, which are based on the original $V_{0\lambda}$ values appear to produce an unusual curve shape. In fact, it seems to underestimate τ_{a340} , but overestimates τ_{a440} . This is particularly pronounced when AOT values are smaller than 0.2 at these short wavelengths, especially for instrument numbers 3761 and 3762. This behavior was previously observed during the analysis of Figures 1a to 1e above. The Langley coefficients show a good spectral behavior. Figure 5 shows that with respect to MLO-calibrated AERONET AOT values, when Microtops Sun photometers are used uncalibrated or calibrated by Langley at a location other than ideal, errors incurred can be of the order of 0.05 at 340 nm and 440 nm, about 0.03 at 675 nm, and 0.02 at 870 nm and 936 nm.

[36] Table 7 shows root-mean-square (rms) values of deviations between the MLO-calibrated AERONET AOT values and three categories of $\tau_{a\lambda}$ and W values for the five Microtops, during the period of the last acceptable calibration for each instrument. The first set of Microtops values is based on the original parameter settings from the Manufacturer. The second set is based on the use of new calibration coefficients $V_{0\lambda}$ (and the new value of $k = 0.615$) substituted into the internal equations of the Microtops (in which τ_{a936} is calculated as $0.91 \tau_{a870}$ and no ozone correction is applied). This is the same as setting the new parameters in the instruments before taking measurements. The third set of RMS values represents recomputation of values based on the standard equations (1) to (4). This is equivalent to post measurement adjustment of values. The first set of RMS values shows that without calibration, three-year old Microtops Sun photometers (being the age of almost all the instruments used) can incur errors in AOT of the order of 0.15 at 340 nm, about 0.08 at 440 nm and 675 nm, down to about 0.02 at 870 nm and 936 nm wavelengths, but errors in W can go as high as 0.8 cm. When calibrated, errors are much lower, the worst cases of AOT RMS being of the order of 0.02 at 340 nm, decreasing to 0.01 at 936 nm, while for water vapor, it is about 0.1 cm. The RMS values for the post calibrated data appear to be slightly better than those potentially obtained by setting the calibration parameters in the instruments, probably because of the slight difference in the Microtops internal equations with respect to the standard equations as used in equations (1) to (4).

5. Conclusions and Recommendations

[37] The measurement characteristics of five Microtops Sun photometers have been investigated during a period of three years to understand the instrument better and to establish its reliability for use in determining aerosol optical thickness and precipitable column water vapor. The experiment was conducted at the NASA Goddard Space Flight Center (GSFC) facility in Greenbelt, Maryland. Measurements were often taken alongside the automatic tracking MLO-calibrated AERONET master Sun photometer, which is believed to be reliable, and therefore used as a standard. The following conclusions may be drawn from the results of the experiment:

1. For accurate AOT determination, Microtops Sun photometers need to be pointed accurately to the Sun, such that the image of the latter is centered correctly in the view window of the instrument. Otherwise, the determined AOT values may become much larger than the true values.
2. Based on their original factory calibration parameters, the five Microtops Sun photometers used in this study tend to underestimate AOT at the ultraviolet wavelength (340 nm) but overestimate it at the visible and near infrared wavelengths (440–936 nm). It is possible that other Microtops with similar characteristics may exhibit the same type of behavior.
3. Regular calibration is essential to maintain high accuracy standards and for monitoring the up-to-date measurement characteristics of Microtops Sun photometers.
4. It is not advisable to perform Langley calibration at a site where aerosol or water vapor concentration may be high

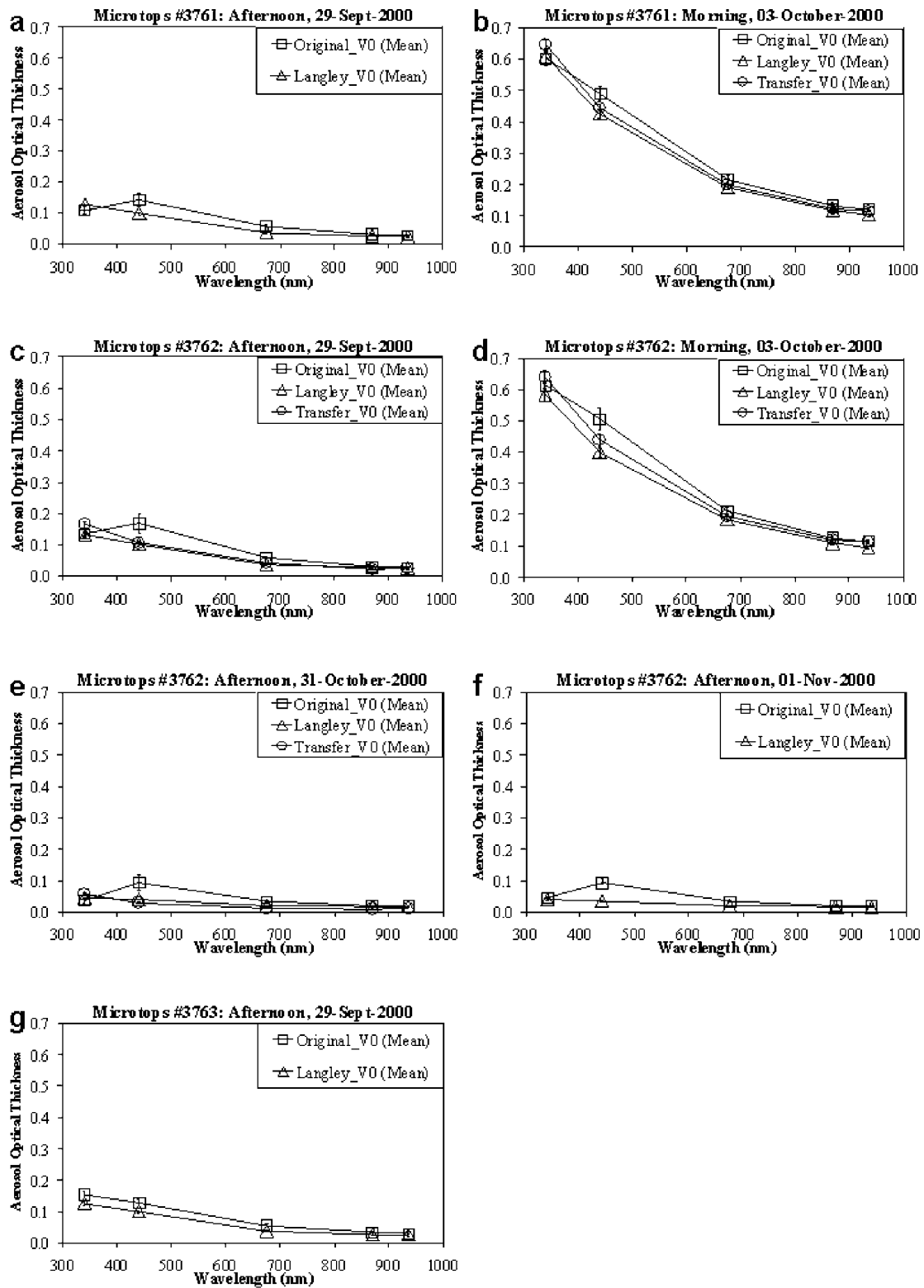


Figure 5. Comparison of spectral plots of mean AOT values based on the original V_0 of the Microtops and those derived from the Langley and transfer calibrations. The plotted values are the mean values for a single session (morning or afternoon) of observations. The error bars represent the standard deviations. The instrument identification number, session, and date of observation are indicated on each panel.

Table 7. Root-Mean-Square (rms) Deviations of AOT and Water Vapor Between the Microtops and AERONET Sun Photometers^a

Serial No.	Instrument ID	Start Date	Stop Date	Data Days	Observations	Variables	AOT_340	AOT_440	AOT_675	AOT_870	AOT_936	Water
1	3761	21-Sep-00	03-Oct-00	5	129	Original	0.067	0.064	0.021	0.017	0.014	0.587
						Cal_Microtops_equ	0.018	0.008	0.013	0.012	0.012	0.080
						Cal_Standard_equ	0.015	0.008	0.006	0.012	0.014	0.064
2	3762	03-Oct-00	31-Oct-00	3	76	Original	0.031	0.088	0.019	0.009	0.005	0.813
						Cal_Microtops_equ	0.013	0.009	0.011	0.002	0.003	0.098
						Cal_Standard_equ	0.008	0.009	0.003	0.002	0.007	0.076
3	3763	01-Jun-00	07-Jun-00	3	42	Original	0.033	0.020	0.014	0.008	0.008	0.738
						Cal_Microtops_equ	0.024	0.008	0.017	0.008	0.008	0.044
						Cal_Standard_equ	0.020	0.008	0.011	0.008	0.008	0.027
4	3760	16-Mar-99	31-Mar-99	3	17	Original	0.022	0.060	0.080	0.026	0.023	0.092
						Cal_Microtops_equ	0.012	0.003	0.014	0.002	0.003	0.034
						Cal_Standard_equ	0.005	0.003	0.002	0.002	0.003	0.016
5	3657	26-Jun-00	07-Jul-00	6	53	Original	0.147	0.034	0.021	0.011	0.011	0.729
						Cal_Microtops_equ	0.020	0.009	0.017	0.011	0.010	0.060
						Cal_Standard_equ	0.017	0.009	0.011	0.011	0.012	0.044

^aThe three sets of rms refer to different categories of Microtops AOT and W : (i) Raw AOT and W values as obtained directly with original parameter settings (Original), (ii) values derived with calibrated V_0 and $k = 0.615$ based on the internal Microtops calibration equations without ozone correction (Cal_Microtops_equ), and (iii) values derived with calibrated V_0 and $k = 0.615$ based on the standard equations (1) to (4) with ozone correction (Cal_Standard_equ).

or variable. If it is not possible to calibrate at such designated areas as the Mauna Loa pristine mountaintop, calibration by transfer of parameters from a more accurate Sun photometer, such as that of AERONET at GSFC, is preferable.

5. It has been found that the Microtops' k instrument constant (as used in equation (2)), set by the manufacturer as 0.7847, is probably wrong, and when used in transfer calibration, causes large fluctuations in V_{0w} heavily correlated with W . This unsteady trend and dependence on water vapor amount makes V_{0w} unreliable. A more accurate value for k has been evaluated to be about 0.615, which makes V_{0w} to behave reasonably well. However, V_{0w} computation based on the modified Langley calibration method is independent of k .

6. The computation of τ_{a936} in the Microtops as 0.91 τ_{a870} is inaccurate. It is recommended that adjusted τ_{a936} be estimated by logarithmic extrapolation from adjusted τ_{a675} and τ_{a870} . Then, the adjusted τ_{a936} may be used to adjust W .

7. The Microtops internal algorithm used in the derivation of $\tau_{a\lambda}$ (and τ_{aw}) does not include correction for ozone. This correction can however be accomplished through post-measurement data adjustment.

8. The front quartz window through which the solar flux gets into the Microtops Sun photometer needs to be cleaned regularly to prevent measurement errors. Lack of such cleaning affects the calibration coefficient $V_{0\lambda}$ (and therefore AOT). This effect is more significant at 340 nm than at any of the other wavelengths.

9. As long as Microtops are properly calibrated regularly (at least once a year) and cleaned frequently, the calibration coefficients $V_{0\lambda}$ are appreciably stable, and decrease very slowly with time. Therefore, the mean of coefficients obtained during any calibration season could be set in the instrument after each calibration season, provided they are accurate. AOT measured with them are expected to meet acceptable standards until the next calibration season.

10. When the Microtops is well calibrated and well cleaned, its AOT retrievals can be of comparable accuracy to those of CIMEL Sun photometers used in the AERONET network, with uncertainties in the range of 0.01 to 0.02 [Holben et al., 2001].

[38] **Acknowledgments.** This research was conducted within the framework of the NASA MODIS aerosol validation project. We received great cooperation from Solar Light Co. (the manufacturer of the Microtops II Sun photometers), particularly Wayne Eckman, who provided us the essential technical information. We would like to thank all the people involved in the AERONET project, especially those dealing with the maintenance and calibration of the master CIMEL Sun photometers located at GSFC. Also, we thank the NASA SIMBIOS Project for its efforts in elaborating and providing the essential algorithm and parameters for computing the aerosol, Rayleigh, and ozone components of the optical thickness.

References

- Bodhaine, B. A., N. B. Wood, E. G. Dutton, and J. R. Slusser, On Rayleigh optical depth calculations, *J. Atmos. Oceanic Technol.*, 16, 1854–1861, 1999.
- Chu, D. A., Y. J. Kaufman, C. Ichoku, L. A. Remer, D. Tanré, and B. N. Holben, Validation of MODIS aerosol optical depth retrieval over land, *Geophys. Res. Lett.*, 29, 10.1029/2001GL013205, in press, 2002.
- Dutton, E. G., P. Reddy, S. Ryan, and J. J. DeLuisi, Features and effects of aerosol optical depth observed at Mauna Loa, Hawaii: 1982–1992, *J. Geophys. Res.*, 99, 8295–8306, 1994.

- Eck, T. F., B. N. Holben, J. S. Reid, O. Dubovik, A. Smirnov, N. T. O'Neill, I. Slutsker, and S. Kinne, Wavelength dependence of the optical depth of biomass burning, urban, and desert dust aerosols, *J. Geophys. Res.*, *104*, 31,333–31,349, 1999.
- Edlén, B., The refractive index of air, *Metrologia*, *2*, 71–80, 1966.
- Goloub, P., D. Tanre, J. L. Deuze, M. Herman, A. Marchand, and F. M. Breon, Validation of the first algorithm applied for deriving the aerosol properties over the ocean using the POLDER ADEOS measurements, *IEEE Trans. Geosci. Remote Sens.*, *37*, 1586–1596, 1999.
- Halothore, R. N., T. F. Eck, B. N. Holben, and B. L. Markham, Sun photometric measurements of atmospheric water vapor column abundance in the 940-nm band, *J. Geophys. Res.*, *102*, 4343–4352, 1997.
- Holben, B. N., et al., AERONET-A federated instrument network and data archive for aerosol characterization, *Remote Sens. Environ.*, *66*, 1–16, 1998.
- Holben, B. N., et al., An emerging ground-based aerosol climatology: Aerosol optical depth from AERONET, *J. Geophys. Res.*, *106*, 12,067–12,097, 2001.
- Ichoku, C., D. A. Chu, S. Mattoo, Y. J. Kaufman, L. A. Remer, D. Tanré, I. Slutsker, and B. Holben, A spatio-temporal approach for global validation and analysis of MODIS aerosol products, *Geophys. Res. Lett.*, *29*, 10.1029/2001GL013206, in press, 2002.
- London, J., R. D. Bojkov, S. Oltmans, and J. I. Kelley, Atlas of the global distribution of total ozone July 1957–June 1967, *NCAR Tech. Note 133+STR*, 276 pp., Natl. Cent. for Atmos. Res., Boulder, Colo., 1976.
- Molina, L. T., and M. J. Molina, Absolute absorption cross sections of ozone in the 185- to 350-nm wavelength range, *J. Geophys. Res.*, *91*, 14,501–14,508, 1986.
- Morys, M., F. M. Mims III, S. Hagerup, S. E. Anderson, A. Baker, J. Kia, and T. Walkup, Design, calibration, and performance of Microtops II handheld ozone monitor and Sun photometer, *J. Geophys. Res.*, *106*, 14,573–14,582, 2001.
- Porter, J. N., M. Miller, C. Pietras, and C. Motell, Ship based sun photometer measurements using Microtops sun photometers, *J. Atmos. Oceanic Technol.*, *18*, 765–774, 2001.
- Reagan, J., K. Thome, B. Herman, R. Stone, J. Deluisi, and J. Snider, A comparison of columnar water-vapor retrievals obtained with near-IR solar radiometer and microwave radiometer measurements, *J. Appl. Meteorol.*, *34*, 1384–1391, 1995.
- Remer, L. A., et al., Validation of MODIS aerosol retrieval over ocean, *Geophys. Res. Lett.*, *29*, 10.1029/2001GL013204, in press, 2002.
- Sabbah, I., C. Ichoku, Y. J. Kaufman, and L. A. Remer, Full year cycle of desert dust spectral optical thickness and precipitable water vapor over Alexandria, Egypt, *J. Geophys. Res.*, *106*, 18,305–18,316, 2001.
- Schmid, B., and C. Wehrli, Comparison of the sun photometer calibration by use of the Langley technique and the standard lamp, *Appl. Opt.*, *34*, 4500–4512, 1995.
- Schmid, B., K. J. Thome, P. Demoulin, R. Peter, C. Mätzler, and J. Sekler, Comparison of modeled and empirical approaches for retrieving columnar water vapor from solar transmittance measurements in the 0.94- μm region, *J. Geophys. Res.*, *101*, 9345–9358, 1996.
- Schmid, B., P. R. Spyak, S. F. Biggar, C. Wehrli, J. Sekler, T. Ingold, C. Matzler, and N. Kampfer, Evaluation of the applicability of solar and lamp radiometric calibrations of a precision Sun photometer operating between 300 and 1025 nm, *Appl. Opt.*, *37*, 3923–3941, 1998.
- Solar Light Company, Inc., User's guide: Microtops II ozone monitor and sunphotometer (version 2.42), *Doc. MTP04*, Sol. Light Co., Philadelphia, Pa., Feb. 2000.
- Teillet, P., Rayleigh optical depth comparisons from various sources, *Appl. Opt.*, *29*, 1897–1900, 1990.
- Vigroux, E., Contribution à l'étude expérimentale de l'absorption de l'ozone, *Ann. Phys.*, *8*, 709–762, 1953.
- Weih, P., I. Dirmhirn, and I. M. Czerwenka-Wenkstetten, Calibration of sunphotometer for measurements of turbidity, *Theor. Appl. Climatol.*, *51*, 97–104, 1995.
- Zhao, T. X.-P., L. L. Stowe, A. Smirnov, D. Crosby, J. Sapper, and C. R. McClain, Development of a global validation package for satellite oceanic aerosol optical thickness retrieval based on AERONET observations and its application to NOAA/NESDIS operational aerosol retrievals, *J. Atmos. Sci.*, *59*, 294–312, 2002.

N. Abuhassan, T. F. Eck, B. N. Holben, and I. Slutsker, Laboratory for Terrestrial Physics, NASA Goddard Space Flight Center, Code 923, Greenbelt, MD 20771, USA.

C. Ichoku, Y. J. Kaufman, R. Levy, R.-R. Li, V. J. Martins, and L. A. Remer, Laboratory for Atmospheres, NASA Goddard Space Flight Center, Code 913, Greenbelt, MD 20771, USA. (ichoku@climate.gsfc.nasa.gov)

C. Pietras, Science Applications International Corporation-General Sciences Corporation, NASA Goddard Space Flight Center, Code 970.2, Greenbelt, MD 20771, USA.